

**SIZE DEPENDENCE FERROMAGNETIC-LIKE BEHAVIOR IN THIOL CAPPED
GOLD NANOPARTICLES.**

J. de la Venta, M. A. Garcia, E. F. Pinel

*Instituto de Magnetismo Aplicado (UCM-ADIF-CSIC) and Depto. Física de Materiales, UCM,
P. O. Box 155, 28230 Las Rozas, Madrid, Spain.*

PACS:

Abstract.

Gold nanoparticles capped with thiols present a surprising ferromagnetic-like behavior despite the diamagnetic behavior of bulk gold. In this work, we study the size dependence of this magnetism and the behavior of these particles. The NPs were characterized by X-ray diffraction and Atomic Force Microscopy. The Surface Plasmon Resonance Band was studied by means of UV-Vis spectroscopy and the magnetic characterization was carried out with SQUID magnetometer. The study reveals that this surprising magnetism, which is highly dependent on the particle size, is located in the outer shell of the NPs, while the core preserves the bulk characteristics.

Text.

In the last years there has been a great interest in the field of nanoscience and nanotechnology. Among these nanosystems, one of the most extensively studied are nanoparticles (NPs). They present novel physical properties¹ and have present and future applications towards biomedicine². The origin of these new properties is two fold: the reduction of size that causes changes in the electronic level of the NPs and the increase in the ratio of surface atoms respect to the volume ones. These superficial atoms have special characteristics, due to the decrease of coordination number, and they may also be joined to different atoms or molecules. These bonds could alter the behavior of the whole system.

One of the most striking examples of new physics that arises at the nanoscale is the discovery of ferromagnetic-like behavior in gold NPs^{3,4} and thin films^{5,6} when they are capped with certain organic molecules, despite the diamagnetic behavior of bulk gold.

In this work we extend this study of the surprising ferromagnetic-like behavior in gold NPs capped with thiols, towards the size dependence of this magnetism.

The chemical synthesis of the NPs consists in the reduction of a metal salt precursor, in a liquid phase, in presence of “protective” species that, due to the formation of covalent links or by electrostatic interactions, isolate the metal cluster preventing its growth.

The thiol capped NPs preparation was done following the well known Brust-Schiffrin method⁷. Briefly, a gold metallic salt, tetrachloroauric(III) acid (HAuCl_4), in aqueous solution is first transferred to an organic medium, toluene with the help of a phase transfer reagent, tetraoctylammonium bromide [$\text{CH}_3(\text{CH}_2)_7$]₄N (Br). In this organic medium, the metallic salt is reduced in presence of a capping molecule, in our case dodecanethiol ($\text{CH}_3(\text{CH}_2)_{11}\text{SH}$).

The particle size is controlled mainly by the molar ratio of the metallic salt respect to the thiol (AuCl_4^- : RSH, named Au:S after here) and also by the temperature of the reaction and the rate of reductant addition⁸. The increase in the amount of thiol produces a decrease in size of the NPs, due to the metallic clusters are rapidly capped for the excess of thiol. In addition, the faster the reductant addition, the narrower the NP size distribution. Consequently, we can achieve a good control over the NP size controlling these parameters.

The figure 1 shows a scheme of a thiol capped Au NP. The particle has two different regions, a metallic core and an outer shell where the thiol chain is joined to the gold via a Au-S bond.

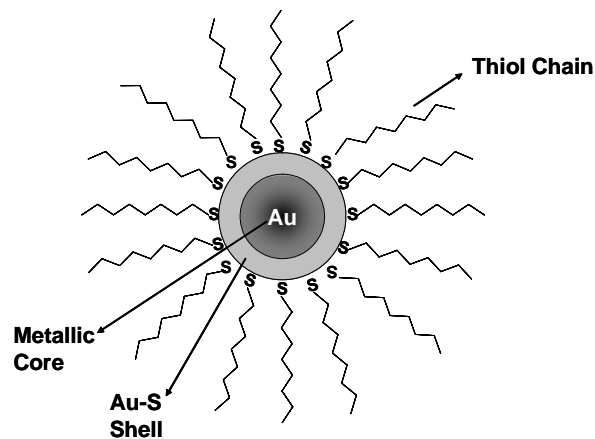


Figure 1. Scheme of a thiol capped Au NP.

We have synthesized three sets of NPs, with molar ratios Au:S, 10:1, 4:1 and 1:1. In a first step the NPs were characterized by X-ray powder diffraction (XRD). Figure 2 shows the diffractograms for the three sets of Au NPs. The broadening of the maxima confirms that there is a decrease in the size when the amount of thiol is increased.

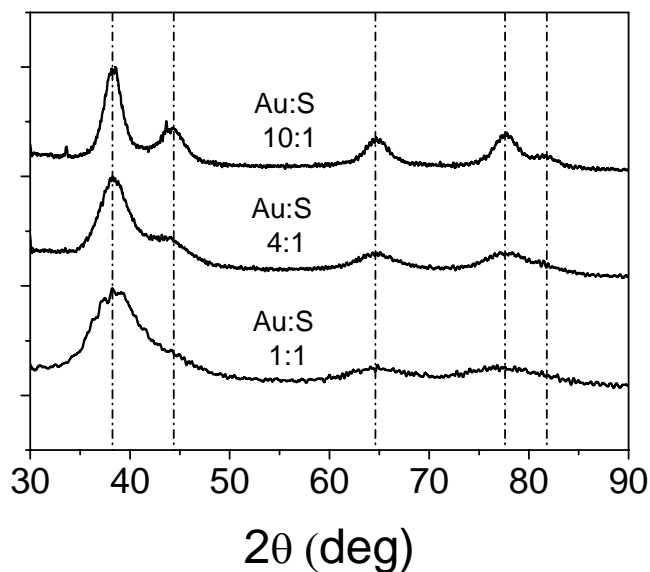


Figure 2. X ray diffractograms of three sets of Au NPs with different Au:S molar ratio. Dashed lines represent the maxima corresponding to a fcc Au unit cell.

This decrease in size is confirmed by atomic force microscopy (AFM). The characterization of NPs with an AFM is not straightforward because we are in the limit of resolution of this technique. The conditions must be optimum and are well described in the literature⁹. It is worth mention that all the information about the size of the NPs must be obtained from the height curves and not from the width, which is larger than the real size of the particles due to the convolution effect between the tip and the NPs. Figure 3a shows an AFM image, in

tapping mode, of NPs with a molar ratio Au:S, 4:1. They have approximately 6 nm of size. Figure 3b shows NPs with molar ratio 1:1, which have approximately 2.5 nm. These sizes agree with those found applying the Debye-Scherrer formula to the diffractograms showed in figure 1.

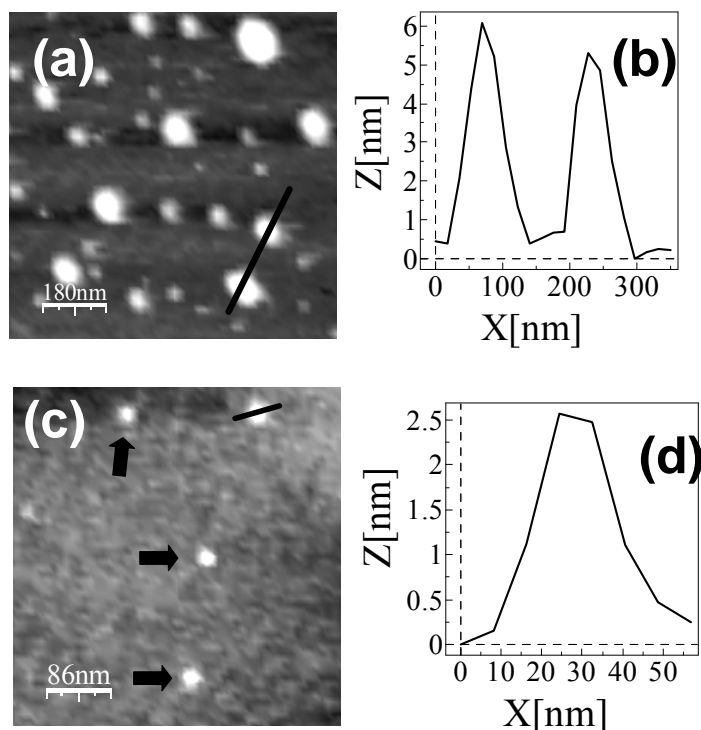


Figure 3. AFM image from Au thiol-capped NPs with different Au:S molar ratio (a) 4:1 and (c) 1:1. The arrows show the isolated NPs. (b) and (d) height profile along the line indicated.

The optical absorption of the NPs has been also studied. The surface plasmon resonance (SPR) is the most remarkable optical property of metallic NPs^{10,11}. It consists on a collective oscillation of the conduction electrons inside the NP. When an external electromagnetic field is applied, an excess of charge arises at the NP surface. This excess of charge acts as a restoring force, while the electron movement is damped mainly because of the electron interactions with atomic cores and NP surface. Hence, the system acts as a damped oscillator which presents a resonance frequency that for most of the transition metals lies on the UV-Vis part of the spectrum¹².

Hence, the NPs exhibit an absorption band in this region of the optical absorption spectrum. According to the Mie theory, as the damping constant depends strongly on the particle size, the shape of the SPR also does. The decrease in size causes the broadening of the absorption band. In fact, for thiol-capped Au NPs smaller than 1.5 nm the band is absent^{3,13}. Figure 4 shows the optical absorption spectra for the two sets of NPs analyzed before. The band is centered in 2.38 eV, i. e. 520 nm of wavelength. The decrease in size is again confirmed by

the broadening of the absorption band. The NPs of 2.5 nm present an absorption band that is clearly broader than that of 6 nm.

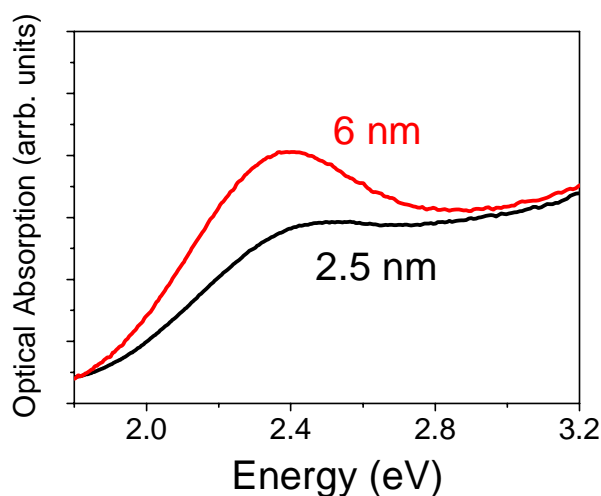


Figure 4. Optical absorption band for thiol capped NPs of 6 nm and 2.5 nm.

But the width of the absorption band is also dependent on the capping molecule. Figure 5 shows the experimental absorption band, after a linear background correction and the calculated data according to the Mie theory. For both cases, the best fit between the experimental data and the calculated absorption occurs when we consider for the theoretical calculation a size which is slightly smaller than the real observed before. For NPs of 2.5 nm, figure 5 a, the best fit is considering NPs of 1.4 nm of size. On the other hand, for the NPs of 6 nm, figure 5 b, experimental and calculated data agree if consider for the calculations a NP size of 4.6 nm instead of the real size.

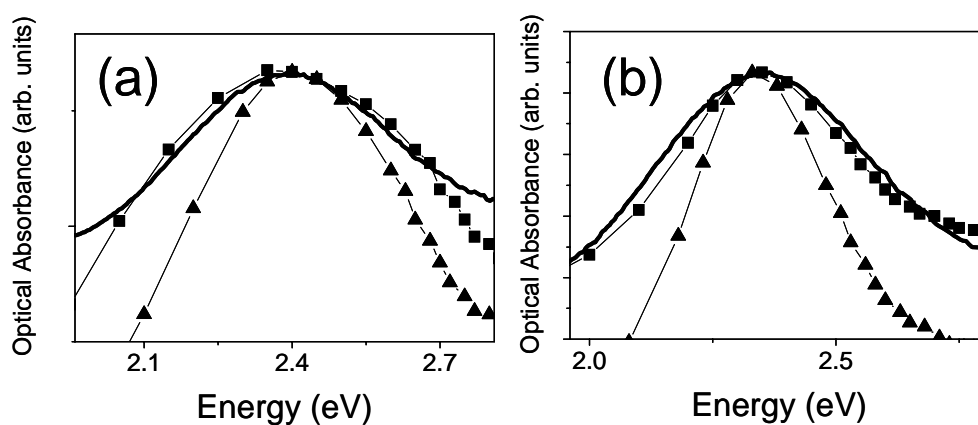


Figure 5. (a) Experimental absorption band (solid line) for thiol-capped AuNPs of 2.5 nm and absorption band according to Mie theory for NPs with sizes of (■) 2.5 nm and (▲) 1.4 nm. (b) Experimental absorption band (solid line) for thiol-capped AuNPs of 6 nm and absorption band according to Mie theory for NPs with radius of (■) 4.6 nm and (▲) 6 nm.

This result is explained by the fact that thiol capped gold NPs have an external shell where the charge is localized, see figure 1. In this region the charge is localized and so the electrons can not oscillate. This produces a decrease in the effective size of the NPs, i. e., the volume of the NP where the electron could oscillate freely. This shell has a size that is estimated in 0.7 nm^3 . This value agrees well with the values obtained in our case, i. e. 0.7 nm for the bigger NPs and 0.6 nm for the case of the smaller. Even, if the NP is small enough, all the electrons are blocked, since the localized charge shell fills all de NP, and this causes the complete extinction of SPR absorption band observed in very small NPs.

The magnetic characterization was carried out with a SQUID magnetometer. The diamagnetic signal of the sample holder have been previously measured and removed from the total magnetization of the sample. Figure 6 shows the measurements of the sample holder and of the NPs of 2.5 nm at different temperatures.

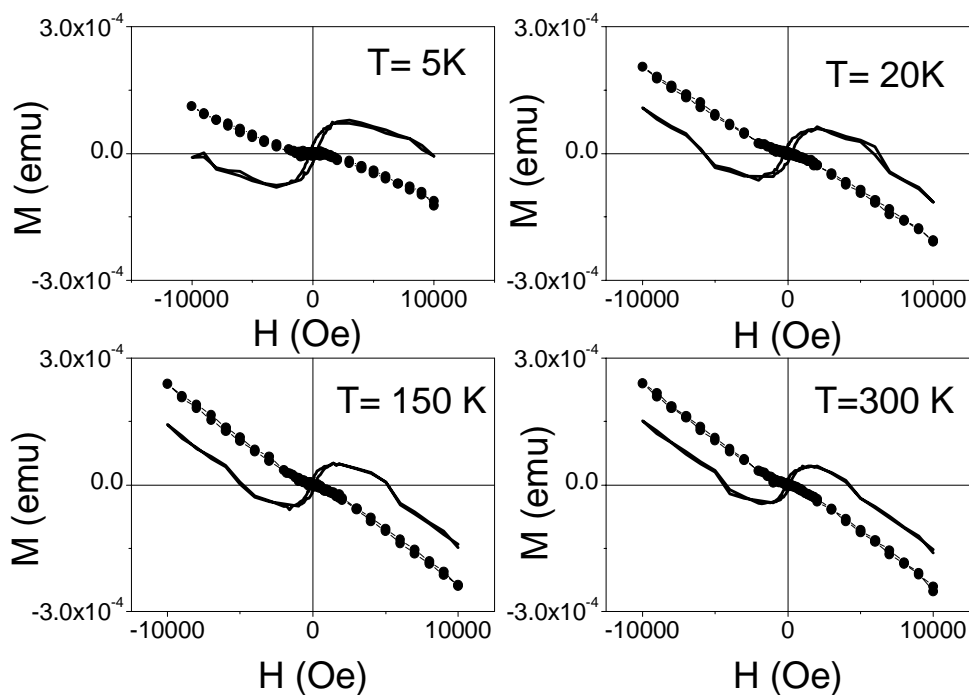


Figure 6. M vs H measurements of the sample holder (●) and thiol capped Au NPs (solid lines) at different temperatures.

It is clear that the diamagnetic signal comes from the holder. In fact, subtracting this signal and normalizing to the amount of gold, we obtain only the contribution from the Au NPs, figure 7. The insets show the coercive field, confirming the presence of hysteresis up to room temperature.

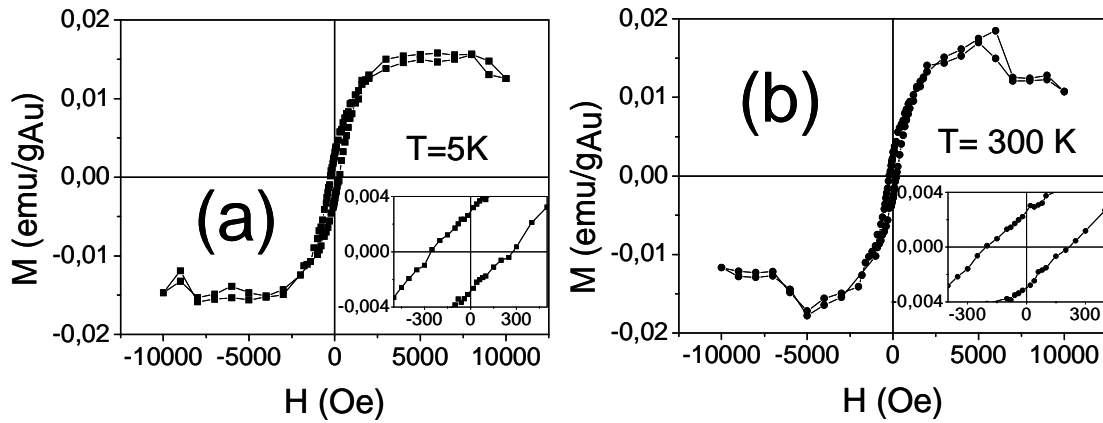


Figure 7. Magnetization curves at different temperatures for thiol-capped Au NPs with 2.5 nm at (a) 5 K and (b) 300 K. The insets show the coercive field.

The surprising ferromagnetic-like behavior observed in thiol capped Au NPs is strongly dependent on the particle size. NPs of 2.5 nm, figure 6, show a ferromagnetic-like behavior with hysteresis up to room temperature, as we have seen before. However, NPs of 6 nm, figure 8 present a diamagnetic behavior for high magnetic fields and a ferromagnetic-like component in the central part of the magnetization curve.

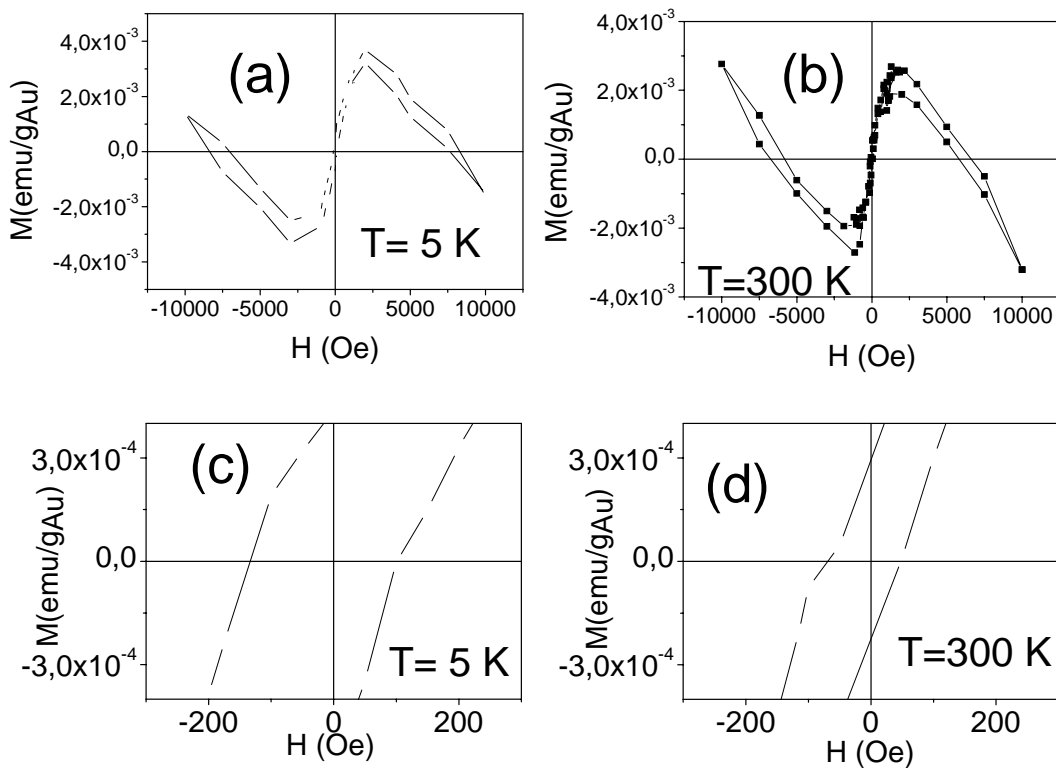


Figure 8. Magnetization curves at (a) 5 K and (b) 300 K for thiol-capped Au NPs of 6 nm and (c), (d) the detail of the coercive force at different temperatures.

To explain this behavior we suggest that the NPs have two different regions as is described in figure 1: the inner metallic core, which presents a diamagnetic behavior similar to bulk gold, and the outer shell (with the Au-S bond), which have a ferromagnetic behavior.

The addition of these two effects gives rise to different magnetic behaviors showed before. In NPs of 6 nm, the diamagnetic contribution is dominant. This is because the strongest contribution is due to the metallic core since the ratio of surface atoms respect from the volume atoms is small. However, in small particles, surface atoms become more important. Therefore, the Au-S shell has a strong contribution, against the metallic core, and the ferromagnetic contribution is the most important.

In fact, if we consider the only the magnetization per surface atom, the values are of the same order of magnitude. This is approximately 0.01 emu per gold atom at the surface for the bigger particles and 0.02 emu per gold atom at the surface for the smaller. The values are not the same due to that there are other factors that could alter the behavior, such as particle size distribution or the efficiency of the Au-S bonds. Taking the diamagnetic part of the hysteresis loops of figure 7, we obtain a value of approximately 5×10^{-7} emu/gOe, which is of the same order of magnitude than the diamagnetic susceptibility of bulk gold, which is $\chi = -1.4 \times 10^{-7}$ emu/gOe. The fact that the values are not equal is attributed to the existence of an extra diamagnetic contribution arising from the thiol chains joined to the Au atoms and perhaps some excess of thiol not bonded to the gold. For the case of bigger nanoparticles, the susceptibility at 300 K is $\chi = 2.68 \times 10^{-7}$ emu/gOe a close value from the bulk.

The thermal dependence of the magnetization, figure 9, is independent of the temperature and is stable even at 300 K, without showing any superparamagnetic behavior, indicating a huge anisotropy.

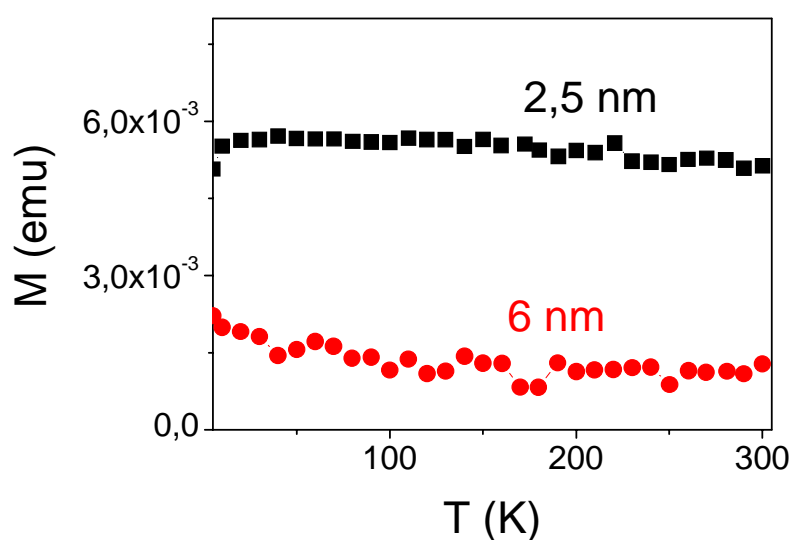


Figure 9. Thermal dependence of the magnetization for NPs of (■) 2.5 nm and (●) 6 nm, under an applied field of 500 Oe.

These results are a clear indication that this magnetism could not be explained by the presence of magnetic impurities, which is always an open question when we are dealing with these systems. As it is well known, magnetic impurities have a magnetization highly dependent on the temperature, which is completely different from our observations. Moreover, the reagents do not contain transition metals that could explain the observed magnetism. Besides, in these nanometer size systems, the impurities should have a superparamagnetic behavior, which is not seen in any measurement. Finally, in recent work¹⁴, the authors show that opposite to what is expected, the presence of magnetic impurities tend to destroy the ferromagnetic behavior and produce changes in the thermal dependence of the energy, which stops being thermal independent and starts to behave thermal dependent. All these facts, allow us to conclude that this surprising ferromagnetic like behavior could not be attributed to the presence of impurities.

A recent explanation has been given to this unexpected ferromagnetism that not only arises in Au NPs but also in thin films^{15,16}. Basically, to explain the ferromagnetic-like behavior we suggest that the thiol chain joins to the gold through the gold-sulphur bond. This produces a charge transfer, as demonstrated the XANES spectra^{3,17}, which gives rise to a magnetic moment. There is also an anisotropy axis in the direction of the thiol chain that in contribution with the spin-orbit coupling produces the blocking of the magnetic moments. Therefore, the charge localization and the anisotropy are responsible for the ferromagnetic-like behavior.

In conclusion, we have synthesized thiol capped NPs with different sizes. The UV-Vis measurements along with the magnetic characterization lead to the conclusion that the surprising ferromagnetic-like behavior is originated in the outer shell of the NPs while the inner core preserves the characteristic of bulk gold.

Acknowledgments

This work has been partially supported by the EU (project "BONSAI" LSHB-CT-2006-037639).

References.

-
1. W. P. Halperin, *Rev. Mod. Phys.*, **58** 533 (1986).
 2. Q.A. Pankhurst et al., *J. Phys. D: Appl. Phys.* **36**, R167-R181. (2003)
 3. P. Crespo et al., *Phys. Rev. Lett* **93** 087204 (2004).
 4. J. de la Venta et al, *Adv. Mater.* In press.
 5. Carmeli et al., *J. Chem. Phys.* **18** 10372 (2003).
 6. A.Hernando et al., *Phys. Rev. B* **74** 052403(2006).
 7. M. Brust, M. Walker, D. Bethell, D. Schiffrin and R. Whyman, *J. Chem. Soc. Chem. Commun.* 801 (1994).
 8. M. J. Hostetler et al., *Langmuir* **14** 17 (1998).
 9. I. Carabias et al., *E-Nano Newsletters* **4** 11 (2006).
 10. U. Kreibig and M. Völlmer, *Optical Properties of Metal Clusters* (Springer-Verlag, Berlin, 1995).

-
11. H. Hövel, S. Fritz, A. Hilger, U. Kreibitz, M. Völlmer, *Phys. Rev. B* **48** 18178 (1993).
 12. J. A. Creighton, D. G. Eadon, *J. Chem. Soc. Faraday Trans.* **87** 3881 (1991).
 13. M. A. Garcia et al., *Phys. Rev. B* **72** 241403(R) (2005).
 14. P. Crespo et al., *Phys. Rev. Lett* **97** 117203 (2006).
 15. A. Hernando, P. Crespo and M. A. Garcia, *Phys Rev. Lett.* **96** 057206 (2006).
 16. A. Hernando et al., *Phys. Rev. B* **74** 052403(2006).
 17. P. Zhang, T. K. Sham, *Phys. Rev. Lett.* **90** 245502 (2003).